

The time-scale for core collapse in spherical star clusters

Gerald D. Quinlan

Lick Observatory, University of California, Santa Cruz CA 95064

Dept. of Physics and Astronomy, Rutgers University, PO Box 849, Piscataway NJ 08855*

September 29, 2018

Abstract

The collapse time for a cluster of equal-mass stars is usually stated to be either 330 central relaxation times (t_{rc}) or 12–19 half-mass relaxation times (t_{rh}). But the first of these times applies only to the late stages of core collapse, and the second only to low-concentration clusters. To clarify how the time depends on the mass distribution, the Fokker-Planck equation is solved for the evolution of a variety of isotropic cluster models, including King models, models with power-law density cusps of $\rho \sim r^{-\gamma}$, and models with nuclei. High-concentration King models collapse faster than low-concentration models if the time is measured in units of t_{rh} , but slower if it is measured in units of t_{rc} . Models with cusps evolve faster than King models, but not all of them collapse: those with $0 < \gamma < 2$ expand because they start with a temperature inversion. Models with nuclei collapse or expand as the nuclei would in isolation if their central relaxation times are short; otherwise their evolution is more complicated. Suggestions are made for how the results can be applied to globular clusters, galaxies, and hypothetical clusters of dark stars in the centers of galaxies.

1 Introduction

The dynamical processes responsible for core collapse are now largely understood (Spitzer 1987). For many star clusters the collapse can be divided into two stages. The first is driven by the approach to thermal equilibrium—a state that is unreachable because of the finite escape velocity. The core contracts to conserve energy as stars evaporate from the high end of the velocity distribution. If this were all that happened the collapse time (called the evaporation time in this context) would be long—a hundred or more half-mass relaxation times. But as the collapse proceeds the core grows hotter and begins transferring energy to the cooler surrounding stars. This causes it to contract further and grow even hotter—an instability known as the gravothermal catastrophe that drives the core in a self-similar manner to zero size and infinite density, with the time remaining until complete collapse at any instant being about 330 times the central relaxation time at that instant. Complications arise near the end when the core is small—stars can merge, massive stars can evolve, binaries can form and harden, possibly stopping and reversing the collapse (reviewed by Goodman 1989, 1993)—but most of the time needed to reach this state is spent near the start where the evolution is simple.

Yet despite the progress that has been made in understanding this evolution, the estimation of collapse times for real star clusters remains confusing. References on the subject usually give two

*Present address.

collapse times. The first, 330 central relaxation times (t_{rc}), applies only to the late, self-similar stage of core collapse. The second, 12–19 half-mass relaxation times (t_{rh}), applies only to low-concentration models like the Plummer model in which the central and half-mass relaxation times are nearly the same. These are poor models for real star clusters. Globular clusters have central relaxation times that are typically ten times shorter than their half-mass relaxation times, sometimes a hundred or a thousand times shorter. Galaxies are even more concentrated: many have densities that continue rising to the innermost observable radius; some have dense nuclear star clusters. Although their half-mass relaxation times are much longer than their ages, their central relaxation times can be short. The simple collapse times quoted above are a poor guide to how relaxation will affect these systems (as Heggie and Mathieu 1986 and Goodman 1993 have stressed).

To broaden the class of models for which core collapse has been studied, this paper uses the Fokker-Planck equation to follow the evolution of a variety of spherical cluster models, including King models (traditionally used to fit globular clusters), a family of models with power-law density cusps of $\rho \sim r^{-\gamma}$ (similar to the cusps observed in galaxies), and some two-component models with nuclei. The calculations are simplified in many ways—the velocity distribution is assumed to be isotropic, the stars are treated as unevolving point masses, all of them having the same mass (except in the models with nuclei), mass loss from a tidal boundary is ignored, binaries are ignored—because the goal is not to study accurate models for real star clusters but to study a wide variety of idealized models and to isolate the dependence of the collapse time on the mass distribution. Binaries and stellar collisions become important only during the late stages of core collapse; the other neglected complications have been studied by others and will not be re-examined here.

The calculations show, as expected, that the simple collapse times quoted above are not applicable to all systems. Low-concentration King models do collapse in about 12–19 t_{rh} , but this is much shorter than 330 t_{rc} for them. High-concentration King models collapse faster than low-concentration models if the time is measured in units of t_{rh} , but slower if it is measured in units of t_{rc} . Models with cusps evolve faster than King models because they start far from thermal equilibrium. But not all of them collapse: those with $\gamma < 2$ undergo a gravothermal expansion because they start with a temperature inversion. Models with nuclei are more complicated: if the nucleus has a short relaxation time it collapses or expands as it would in isolation; otherwise its evolution is determined its interaction with the rest of the model.

The final section of the paper discusses possible applications of the results to globular clusters, galaxies, and hypothetical clusters of dark stars in the centers of galaxies. One technical detail is discussed in an appendix: the variation of the Coulomb logarithm with position. This changes the evolution times only slightly if the number of stars is large, but it can be important for detailed comparisons of Fokker-Planck calculations with N-body experiments.

2 Computational method

2.1 The Fokker-Planck equation

The Fokker-Planck equation describes the evolution of a stellar distribution function resulting from weak two-body encounters, which are more important than strong encounters by a factor of order $\ln N$ when the number of stars N is large. Although the equation can be written for any cluster geometry and any distribution function, its practical solution requires some simplifying assumptions to be made. The calculations done here assume the cluster to be spherical and the distribution function to depend only on energy (so the velocity distribution is isotropic); the diffusion coefficients are evaluated in the local approximation and the equation is orbit averaged (Binney and Tremaine

1987). It then takes the form (Spitzer 1987)

$$\frac{\partial f}{\partial t} - \frac{1}{p} \frac{\partial q}{\partial t} \frac{\partial f}{\partial E} = \frac{1}{p} \frac{\partial}{\partial E} \left(D_E f + D_{EE} \frac{\partial f}{\partial E} \right), \quad (1)$$

where the coefficients D_E and D_{EE} are

$$D_E(E) = 16\pi^2 G^2 m^2 \ln \Lambda \int_{\phi_c}^E dE_1 f_1 p_1, \quad (2)$$

$$D_{EE}(E) = 16\pi^2 G^2 m^2 \ln \Lambda \left(\int_{\phi_c}^E dE_1 f_1 q_1 + q \int_E^{\phi_\infty} dE_1 f_1 \right), \quad (3)$$

and the phase-space integrals p and q are

$$p(E) = \frac{\partial q}{\partial E}, \quad q(E) = \frac{1}{3} \int_0^{\phi^{-1}(E)} dr r^2 [2E - 2\phi(r)]^{3/2}. \quad (4)$$

The density and potential are computed from the distribution function by

$$\nabla^2 \phi(r) = 4\pi G \rho(r) = 16\pi^2 G m \int_{\phi(r)}^{\phi_\infty} dE f [2E - 2\phi(r)]^{1/2}; \quad (5)$$

ϕ_c and ϕ_∞ are the values of the potential at $r = 0$ and $r = \infty$ (ϕ_∞ is assumed to be zero in the rest of the paper). The Coulomb logarithm $\ln \Lambda$ is treated as a constant. Its value—usually taken to be $\ln(kN)$ with some numerical coefficient k of order unity—need not be specified here because it can be absorbed into the unit of time (the relaxation time). The changes that result when $\ln \Lambda$ varies with position are explored in the Appendix.

The assumption that the distribution function depends only on energy is of course not correct: even if it is for the initial model, anisotropy will develop as the evolution proceeds. The Fokker-Planck equation can be solved with a distribution function that depends on both energy and angular momentum, but the calculations are then much more difficult. Calculations done in this way for the collapse of an isotropic Plummer model show that the velocity distribution remains nearly isotropic in the core (Cohn 1985, Takahashi 1995). A radial anisotropy develops in the outer parts of the cluster. This is important for some aspects of the evolution, especially for the escape of stars, but it does not cause a big change in the collapse time. Takahashi's calculation shows the late, self-similar stage of core collapse to be about 40% slower when anisotropy is included; earlier calculations had suggested that it was 40% faster.

The other assumptions made in deriving equation (1)—the orbit averaging, the local approximation, the neglect of close encounters—are difficult to justify (Goodman 1983 modified the equation to include close encounters and found that it did not change the evolution much). Yet the predictions for core collapse made with these assumptions agree well with the results from large N-body experiments (Spurzem and Aarseth 1996). Surprisingly, even experiments with small values of N follow the predictions when many experiments are averaged to reduce the noise (Giersz and Heggie 1994). There are some differences but the agreement is impressive.

2.2 Numerical solution

The Fokker-Planck program of Quinlan and Shapiro (1989) was modified for these calculations so that it could use models with density cusps. It is based on the algorithm developed by Cohn (1980). Since the goal was to compute accurate collapse times, the time steps, grid spacings, and tolerance parameters were chosen smaller than is necessary for most applications. Those choices are described here along with some test results.

The radial grid points were spaced equally in $\log(r)$ between inner and outer boundaries r_{\min} and r_{\max} ($r_{\min} \simeq 10^{-6}$ and $r_{\max} \simeq 10^3$; the exact numbers depend on the model). Most calculations used $\Delta \log(r) = 0.05$; some used a smaller spacing for higher accuracy. For initial models with cores the energy grid points were chosen as in Cohn's program; for models with cusps they were chosen to match the potential at the radial grid points (the number of radial and energy grid points was the same). The equation was advanced with Crank-Nicholson time differencing and Chang-Cooper space differencing; zero-flux boundary conditions were imposed at the inner and outer grid points. The time step for the potential recomputation was chosen so that the central density changed by at most one percent between time steps; 32 Fokker-Planck steps were taken for each potential step. The recomputation was iterated until the potential converged to one part in 10^5 at all grid points (which usually took 8–10 iterations). The phase-space integrals p and q were computed to an accuracy of about one part in 10^5 .

The ability of the program to reproduce the density and potential of the initial models was checked; it did this to at least one part in 10^4 at all grid points (except for the last few near the outer boundary). The main test was the standard Plummer-model collapse. This was followed until the central density had risen by a factor of 10^7 , using 140 grid points with $r_{\min} = 5 \times 10^{-5}$ and $r_{\max} = 500$. Energy was conserved to one part in 10^3 and mass to one part in 10^5 . The collapse time was $15.4 t_{\text{rh}}$. The results for the evolution of the collapse rate, $\xi = t_{\text{rc}} d \ln \rho_c / dt$, the equation of state, $d \ln v_c^2 / d \ln \rho_c$, and the scaled central potential, $x_0 = 3|\phi_c|/v_c^2$, agreed well with those published by Cohn (1980).

3 Results

3.1 Notation

Some definitions and conventions used throughout are gathered here for convenience. The local and half-mass relaxation times are computed from the standard definitions (Spitzer 1987)

$$t_{\text{r}} = \frac{0.065v^3}{G^2 m \rho \ln \Lambda}, \quad (6)$$

$$t_{\text{rh}} = \frac{0.138N}{\ln \Lambda} \left(\frac{r_h^3}{GM} \right)^{1/2}, \quad (7)$$

where $M = Nm$ is the total mass, ρ the density, v the three-dimensional velocity dispersion, r_h the half-mass radius, and $\ln \Lambda$ the Coulomb logarithm. The half-mass relaxation time does not change by much during the evolution of the models studied here; t_{rh} will always denote its initial value. The central relaxation time t_{rc} is given by equation (6) with ρ and v replaced by ρ_c and v_c . The subscript “c” indicates that a variable is to be evaluated at the center; one exception is r_c which denotes the core radius (sometimes called the King radius)

$$r_c = \left(\frac{3v_c^2}{4\pi G \rho_c} \right)^{1/2}. \quad (8)$$

If the units of measurement are not explained when results are presented in the figures or text then they are the standard N-body units in which $G = M = -4E = 1$ (Heggie and Mathieu 1986).

3.2 Models with cores

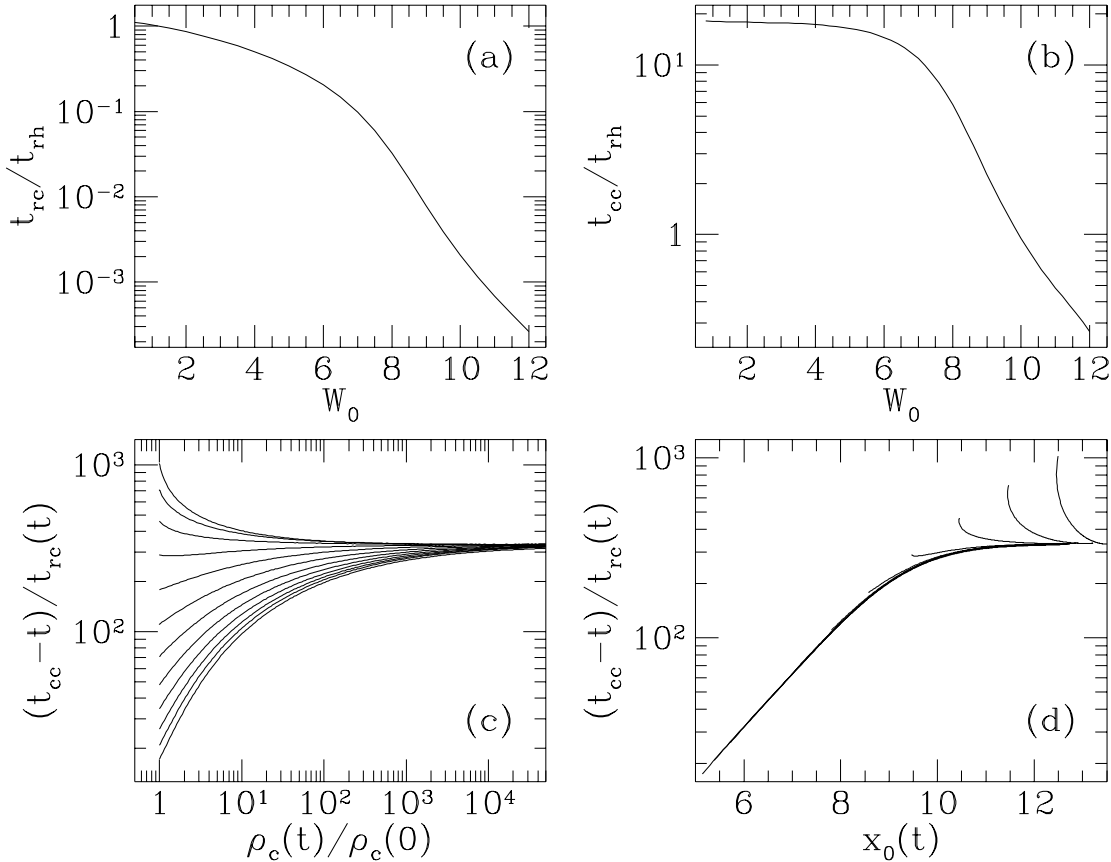


Figure 1: Collapse of isolated King models: (a) ratio of initial central and half-mass relaxation times; (b) collapse time; (c) time remaining until complete collapse during the evolution of twelve models ($W_0 = 1, 2, \dots, 12$, increasing from bottom to top); (d) the same as in (c) but plotted versus $x_0 = 3|\phi_c|/v_c^2$.

3.2.1 Initial models

King models (King 1966) provide a convenient one-parameter family of models with cores. They are lowered isothermals with two length scales: a tidal radius r_t , at which the density drops to zero, and a core radius r_k (which differs slightly from r_c because its definition uses $3\sigma^2$ instead of v_c^2). The concentration is measured by either the parameter $c = \log(r_t/r_k)$ or the dimensionless central potential W_0 , which will be used here; the relation between the two is plotted in Figure 4.10 of Binney and Tremaine (1987). The ratio of the central and half-mass relaxation times varies by nearly a factor of 10^4 over the range $W_0 = 1-12$ (see Fig. 1). In the limit of infinite concentration the King models approach the isothermal sphere.

Two Fokker-Planck studies have followed the collapse of King models: Wiyanto, Kato, and Inagaki (1985) used equal-mass models with $W_0 = 0.5, 6.6$, and 12.2 ; Chernoff and Weinberg (1990) used models with $W_0 = 1, 3$, and 7 , including a distribution of masses and stellar evolution. Both these studies assumed the models to be tidally truncated, meaning that stars were removed if they moved outside the tidal radius and that the tidal radius was reduced along with the mass as $r_t \sim M^{1/3}$. In contrast to these, the present study considers a wide range of concentrations but ignores mass loss: the models are isolated and stars remain bound if they move outside the tidal radius. Mass loss from a tidal boundary reduces the collapse time (because it lowers N while keeping the mean density fixed, which lowers the relaxation time), but this is important only for low-concentration

W_0	c	$t_{\text{rc}}/t_{\text{rh}}$	$t_{\text{cc}}/t_{\text{rc}}$	$t_{\text{cc}}/t_{\text{rh}}$
1.0	0.296	1.032123	18.	18.12
2.0	0.505	0.859156	21.	17.94
3.0	0.672	0.678293	26.	17.70
4.0	0.840	0.502196	34.	17.33
5.0	1.029	0.341928	48.	16.45
6.0	1.255	0.205136	71.	14.56
7.0	1.528	0.098544	110.	10.90
8.0	1.833	0.032641	179.	5.84
9.0	2.118	0.007875	289.	2.28
10.0	2.350	0.002066	459.	0.95
11.0	2.548	0.000683	707.	0.48
12.0	2.739	0.000261	1018.	0.27

Table 1: Collapse times for isolated King models (accurate to about one percent).

models.

The Fokker-Planck program used here required the density to be non-zero at all grid points. The King models were therefore modified at grid points $r \geq r_t$ so that the density fell to a small value at r_t and then continued to fall with radius out to infinity. The mass added in this way was tiny and did not affect the collapse times.

3.2.2 Evolution

Each model was integrated until its core radius r_c had shrunk to 10^{-5} ; by then the central density is much higher and the evolution time-scale much smaller than at the start. An extrapolation was made to predict the time t_{cc} at which r_c would reach zero. These collapse times are plotted in panel (b) of Figure 1 in units of the half-mass relaxation time (see also Table 1). For low-concentration models ($W_0 \leq 7$) they agree with the often-quoted collapse time of $12\text{--}19 t_{\text{rh}}$; for high-concentration models they are shorter.

Panel (c) plots for twelve models the time remaining until complete collapse at any instant during the evolution, $\tau = t_{\text{cc}} - t$, in units of the central relaxation time at that instant. The abscissa is chosen to separate the models; it obscures the fact that the King models form an evolutionary sequence (King 1966, Cohn 1980, Wiyanto et al. 1985). This is clearer in panel (d) where the times are plotted versus the scaled central potential x_0 : the lines for $W_0 = 1\text{--}7$ fall on top of each other, showing that low-concentration King models evolve through states resembling models with higher concentrations; around $W_0 \simeq 7\text{--}8$ the lines depart from this evolutionary sequence, near the value $W_0 = 7.4$ at which King models become unstable to the gravothermal catastrophe (Katz 1980). Deep into the collapse the values of τ/t_{rc} for all the models converge to $\tau/t_{\text{rc}} \simeq 330$, the same value found by Cohn (1980) for the late, self-similar stage of the collapse of a Plummer model. But most of the time is spent near the start where $t_{\text{cc}}/t_{\text{rc}}$ can be quite different from 330: it is much smaller for low-concentration models, and larger for high-concentration models—about 1000 for $W_0 = 12$ and 2500 for $W_0 = 15$ (this last value is not shown in the figure).

The high-concentration King models have long collapse times (when measured in units of t_{rc}) because they are nearly isothermal; other high-concentration models with cores have shorter collapse times. Consider the two models in Figure 2. They have densities $\rho(r) \sim (r^2 + b^2)^{-\gamma}(r + a)^{4-\gamma}$, with a and b chosen to give a concentration like that of the $W_0 = 12$ King model (this is the γ model

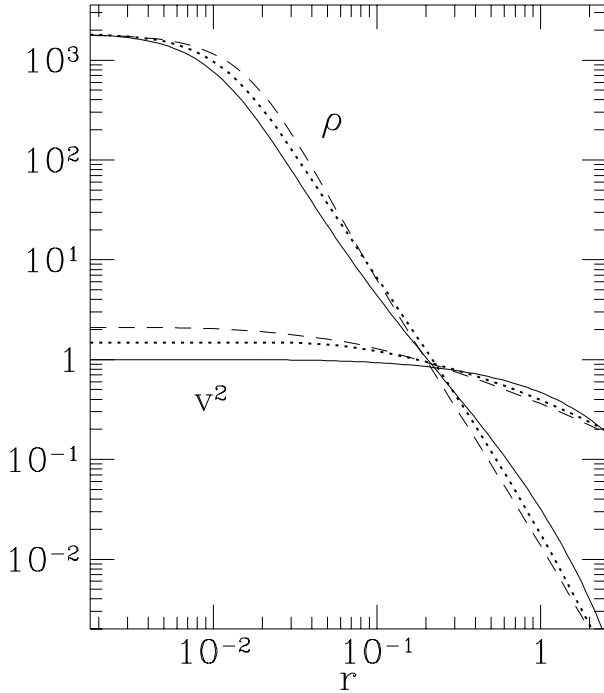


Figure 2: Density and velocity dispersion (squared) for the $W_0 = 12$ King model (solid lines) and for models with $\rho \sim r^{-2.25}$ (dotted) and $\rho \sim r^{-2.5}$ (dashed).

density from the next section, modified to have a core of radius $r_c \simeq b$). The model with $\gamma = 2.25$ collapses in about 400 central relaxation times; the model with $\gamma = 2.5$ in about 100, ten times faster than the $W_0 = 12$ King model.

The amount by which mass loss from a tidal boundary reduces the collapse time can be judged from the results of Chernoff and Weinberg (1990). They give the collapse time for an equal-mass model without stellar evolution for only one concentration ($t_{\text{cc}} = 10.1 t_{\text{rh}}$ for $W_0 = 7$); times for two other concentrations were kindly provided by M. Weinberg (9.6 t_{rh} for $W_0 = 3$ and 2.23 t_{rh} for $W_0 = 9$). The ratios of their times and those found here are 0.54, 0.93, and 0.99 for $W_0 = 3, 7$, and 9. Thus mass loss can reduce the collapse time by about a factor of two for a low-concentration model like the $W_0 = 3$ King model (which loses 75% of its mass during the collapse), but it does not reduce the time by much for high-concentration models.¹

3.3 Models with cusps

¹The collapse times of Wiyanto et al. (1985) are questionable (note that their definition of t_{rc} differs from the definition used here). Their time for $W_0 = 0.5$ is about three times shorter than found here, which seems reasonable, but their times for $W_0 = 6.6$ and 12.2 are longer than found here, by factors of 1.3 (for $W_0 = 6.6$) and 2.6 (for $W_0 = 12.2$). They do not describe the accuracy of their integrations. The integrations done here were repeated with finer grid spacings and smaller time steps and tolerance parameters to check that the times had converged. This required higher accuracies for the high-concentration models than for the low-concentration models.

3.3.1 Initial models

A simple one-parameter family of models with density cusps is provided by the density (Carollo 1993, Dehnen 1993, Tremaine et al. 1994)

$$\rho(r) = \frac{3-\gamma}{4\pi} \frac{Ma}{r^\gamma (r+a)^{4-\gamma}}. \quad (9)$$

In standard N-body units the length scale is $a = 1/(5-2\gamma)$. These will be called γ models; they include as special cases the models of Hernquist (1990), $\gamma = 1$, and Jaffe (1983), $\gamma = 2$. For most γ values the distribution function must be computed numerically from Eddington's formula. The γ models are themselves special cases of a more general family considered by Zhao (1996),

$$\rho(r) = \frac{C}{r^\gamma (r^{1/\alpha} + a)^{(\beta-\gamma)\alpha}}, \quad (10)$$

which resembles the fitting formula used by Lauer et al. (1995) and Byun et al. (1996) for the central regions of elliptical galaxies (but they fit the surface brightness, not the density). The extra flexibility provided by α and β is not needed here because the goal of the calculations is to understand how relaxation affects the central region; that is determined primarily by γ .

The velocity dispersion near the center of a γ model varies with radius as $v^2 \sim r^\gamma$ if $\gamma < 1$ and as $r^{2-\gamma}$ if $\gamma > 1$. The models with $\gamma < 2$ have a temperature inversion: the maximum of v^2 is not at the center (“temperature” and “ v^2 ” can be used synonymously when the stars all have the same mass). This property is shared by all isotropic models with density cusps more gradual than r^{-2} (Binney 1980). Relaxation tends to even out the temperature in a star cluster; energy therefore flows into the center when there is an inversion, causing the central region to expand. This is familiar from Fokker-Planck studies of the post-collapse evolution of globular clusters: the collapse is stopped by something that heats the core (usually binaries), either directly (by increasing the kinetic energy of the stars) or indirectly (by ejecting mass from the core); once the core expands a little it becomes cooler than the surrounding medium and can continue expanding even if the heat source is turned off—the expansion is then said to be gravothermal. Heggie, Inagaki, and McMillan (1994) verified that an N-body system expands when it starts with an inversion like that expected for globular clusters after core collapse; the larger N-body experiments of Makino (1996) show that binaries can produce the required inversion and can cause alternating periods of contraction and expansion known as gravothermal oscillations. The γ models do not need a heat source to start the expansion because they start with a temperature inversion.

The rising density and (for $\gamma < 2$) falling velocity dispersion near the center of a γ model cause a rapid fall in the relaxation time (see Fig. 3), with $t_r \sim r^{5\gamma/2}$ for $\gamma < 1$ and $\sim r^{3-\gamma/2}$ for $\gamma > 1$ (the fastest fall occurs for the Hernquist model). This causes obvious problems for the Fokker-Planck program: the evolution is arbitrarily fast near the center and the zero-flux boundary condition cannot be satisfied. The problems can be avoided by replacing the $r^{-\gamma}$ in the density law by $(r^2 + b^2)^{-\gamma/2}$ to give the models a small core (the experiments described below used $b = 10^{-5}$). The models with $\gamma < 2$ would develop cores in any case once the expansion begins, so it does no harm to give them one at the start provided that b is smaller than the length scales of interest. The models with $\gamma \geq 2$ are not considered here because they do not have temperature inversions and do not expand; if given a core of size b they collapse in a time determined by b , as happened for the two models in Figure 2.

3.3.2 Evolution

The results from the Fokker-Planck calculations show that the models with $\gamma < 2$ expand gravothermally, as expected (see Figs. 4 and 5). They develop cores that grow outward, with the central

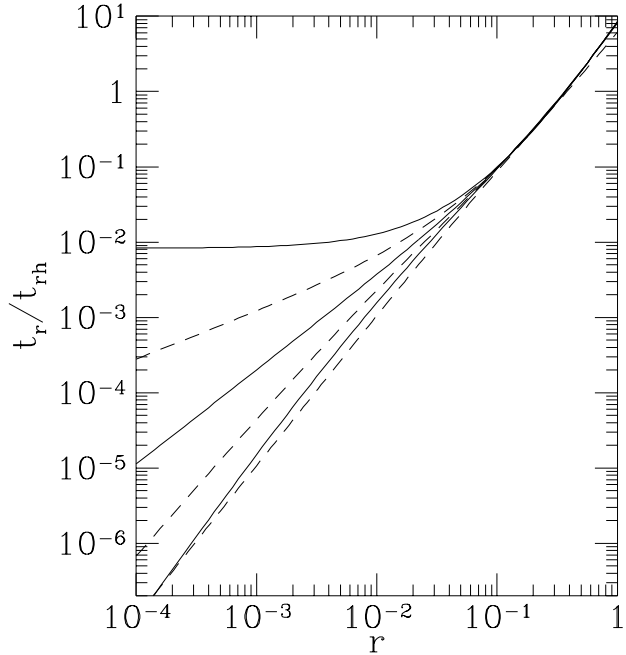


Figure 3: The local relaxation time in γ models with $\gamma = 0.0$ (top line, solid), 0.25 (dashed), 0.5 (solid), 0.75 (dashed), 1.0 (solid), and 2.0 (bottom line, dashed).

density falling and the velocity rising (the outer parts contract slightly to conserve energy). The expansion continues until the temperature inversion is gone; then it reverses and the core collapses. The time to reach complete collapse from the start gets shorter as γ approaches 2 (and the extent of the expansion gets smaller), but it is always long if t_{rh} is long.

The expansion time is more interesting than the collapse time for these models. In the first three panels of Figure 4 (the models with $\gamma \leq 1.5$) the solid lines near the center rise noticeably before they cross the dotted line, showing that the local expansion time is no longer than the relaxation time, unlike in globular clusters where the expansion time after core collapse is usually a thousand or more relaxation times (e.g. Heggie and Ramamani 1989). Another measure of the expansion rate is plotted in Figure 6: $|\xi|$ is of order unity for the γ models with $\gamma \lesssim 1$, much larger than the values of $|\xi| \lesssim 10^{-3}$ typical for globular clusters undergoing gravothermal oscillations (see Fig. 2 of Cohn, Hut, and Wise 1989). The reason the γ models expand so fast is that they start far from thermal equilibrium. As γ approaches 2 the initial temperature inversion gets weaker and the expansion gets slower.

Other isotropic models with power-law density cusps will expand in about the same way as the γ models. The Zhao models with $0 < \gamma < 2$, for example, all have temperature inversions; the parameters α and β will modify the extent of the expansion but not its initial speed.

3.4 Models with nuclei

King models and γ models do not exhaust the possibilities for spherical star clusters. Some galaxies have density cusps that steepen near the center; others have dense cores embedded in larger cores or weak cusps. Lauer et al. (1995) describe these as galaxies with nuclei. Their evolution cannot be surveyed with a simple one-parameter family of models, but it can be described easily in two limits. If the nucleus has a short relaxation time, it collapses or expands as it would in isolation; if it consists of low-mass stars with a long relaxation time, it traps the more massive stars from the

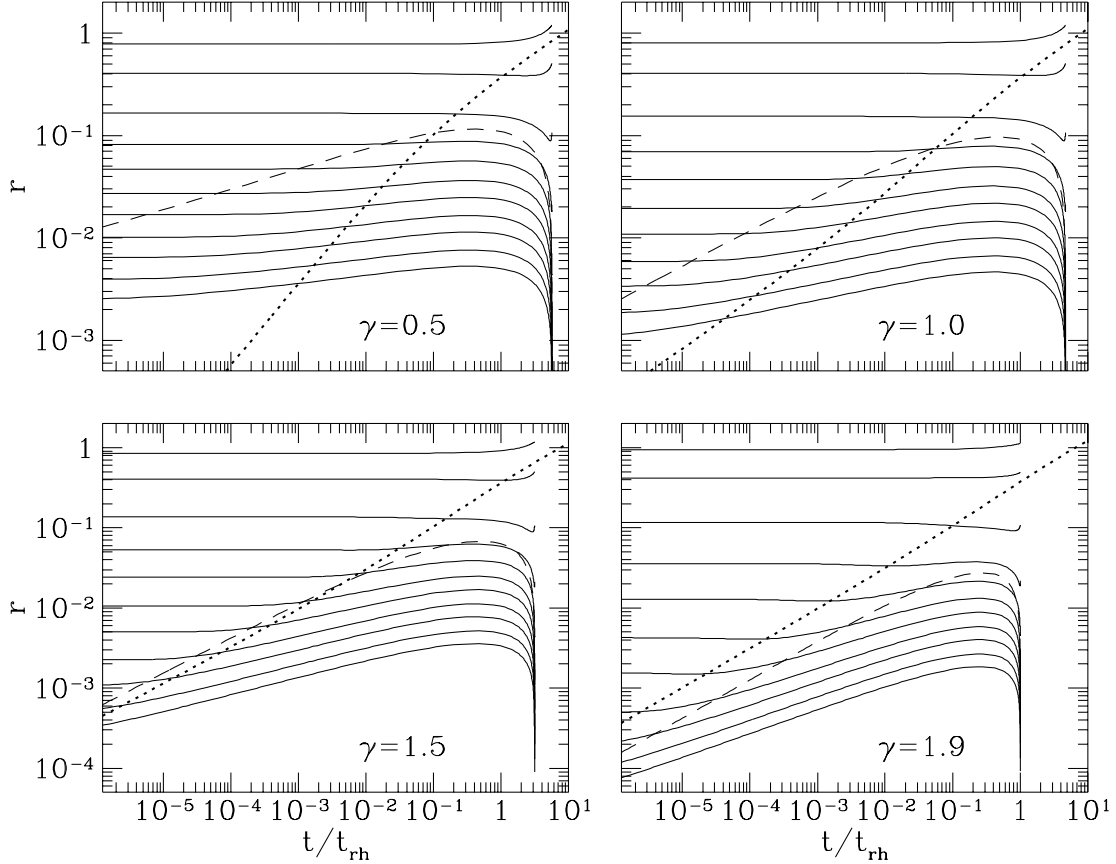


Figure 4: Expansion and collapse of γ models. The solid lines are radii containing fixed fractions of the total mass ($10^{-5}, 3 \times 10^{-5}, 10^{-4}, 3 \times 10^{-4}, \dots, 0.1, 0.3, 0.5$); the dashed line is the core radius. The dotted line shows the local relaxation time versus radius in the initial model.

rest of the galaxy and causes them to collapse. Examples of both limits are described below.

3.4.1 Equal-mass models

A nucleus with a short relaxation time can collapse even if its temperature is lower than the temperature outside the nucleus. As a simple example, consider a model whose density is the sum of two Plummer-model densities, an inner model with mass M_1 and radius R_1 and an outer model with mass M_2 and radius $R_2 > R_1$ (the Plummer potential is $\phi = -GM/\sqrt{r^2 + R^2}$). If $M_1/R_1^3 > M_2/R_2^3$ the inner model has a higher density than the outer model and appears as a nucleus. Yet if $M_1/R_1 < M_2/R_2$ the inner model has a lower temperature than the outer model; whether it collapses or expands then depends on whether its collapse time is shorter or longer than the time for it to absorb energy from the outer model. Figure 7 shows models on the two sides of this boundary: the one with $M_1 = 8 \times 10^{-4}$ collapses despite its temperature inversion; the one with $M_1 = 7 \times 10^{-4}$ collapses at first but then stops and expands. Experiments like this were done for models with $0.005 \leq R_1/R_2 \leq 0.08$; the boundary between the collapsing and expanding models is fit well by $M_1/M_2 = 1020(R_1/R_2)^{3.6}$ over this range. If M_1 is just a few times larger than the boundary then the collapse time is about the same as for an isolated Plummer model ($33 t_{rc}$).

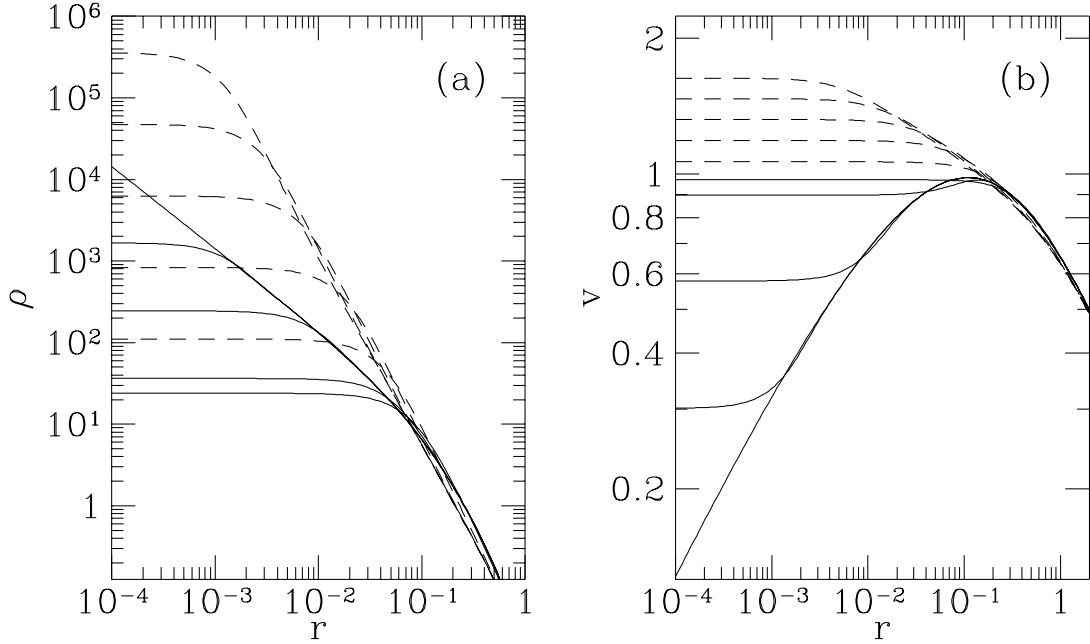


Figure 5: Density and velocity dispersion at ten times during the expansion (solid lines) and collapse (dashed lines) of a Hernquist model ($\gamma = 1$). The first solid line (the highest for ρ , the lowest for v) shows the initial model; the last shows the point of maximum expansion.

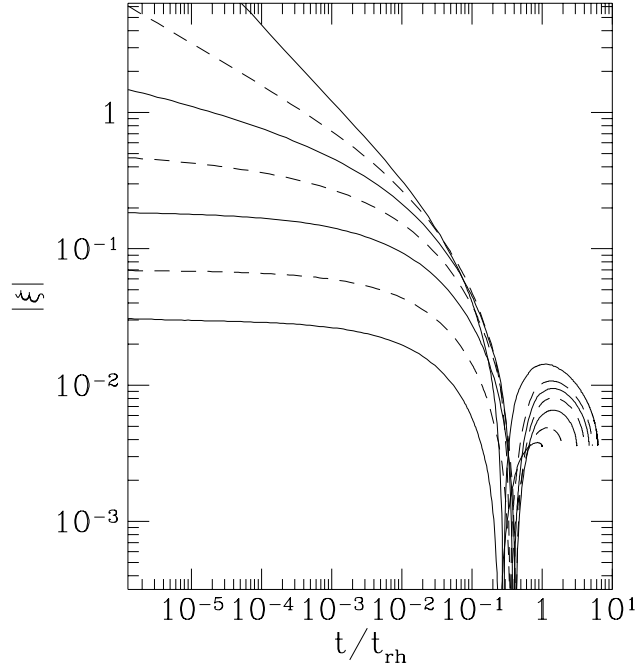


Figure 6: Evolution of $\xi = t_{rc} d \ln \rho_c / dt$ for models with $\gamma = 0.0$ (solid, top line), 0.75 (dashed), 1.0 (solid), 1.25 (dashed), 1.5 (solid), 1.75 (dashed), and 1.9 (solid, bottom line). ξ is negative at first, then changes to positive.

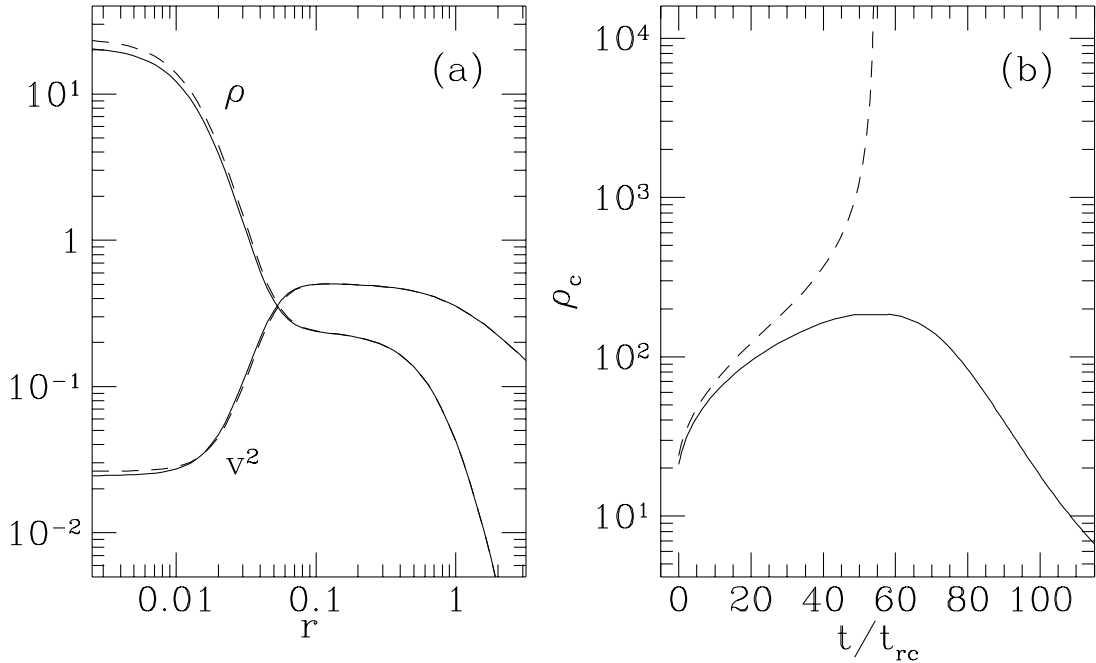


Figure 7: Models with nuclei formed by combining the densities of Plummer models with radii $R_1 = 0.02$ and $R_2 = 1.0$ and masses M_1 and $M_2 = 1 - M_1$: (a) initial density and squared velocity dispersion for $M_1 = 7 \times 10^{-4}$ (solid lines) and 8×10^{-4} (dashed lines); (b) evolution of the central density for the two models (t_{rc} is the initial central relaxation time).

3.4.2 Two-component models

The collapse time for a nuclear star cluster can be lengthened by lowering the mass m_1 of its stars, because $t_{rc} \sim 1/m_1$ when the density is held fixed. But the more massive stars from the rest of the galaxy that pass through the nucleus then get trapped by dynamical friction in a time that is independent of m_1 . This is of interest for models of galaxies with central mass concentrations, for which dark clusters of low-mass stars (which might be brown dwarfs or planets or small black holes) are sometimes proposed as alternatives to massive black holes.

The simple model used in Figure 7 cannot be used to illustrate this limit because its distribution function cannot be split into positive functions f_1 and f_2 that generate the densities of the two Plummer models, for the same reason that Tremaine et al. (1994) could not find positive distribution functions for γ models with central black holes when $\gamma < 1/2$. Instead we shall consider the more realistic model in Figure 8 that has a Plummer-model nucleus embedded in a γ model with $\gamma = 1$. If the two components have equal stellar masses ($m_1 = m_2$) the nucleus collapses independently of the γ model, in about the same time as for an isolated Plummer model. Panel (b) shows what happens when the stellar mass is 100 times smaller in the nuclear component than in the γ -model component. The inner parts of the γ model sink to the center and collapse in a time of about $0.3 t_{rc}$, 100 times shorter than the collapse time for the nucleus if it were isolated.

Experiments with other values of M_1 , R , and γ gave similar results when $m_2/m_1 \gg 1$. The stars of the γ model that start within the nucleus collapse in a time that is m_2/m_1 times shorter than the collapse time for the nucleus if it were isolated. Additional stars will be captured on longer time scales as they get scattered into loss-cone orbits that bring them into the nucleus. The mass that collapses could be reduced by removing stars from the center of the γ model, which would require an anisotropic distribution function with a circular bias near the center, but such a model would be

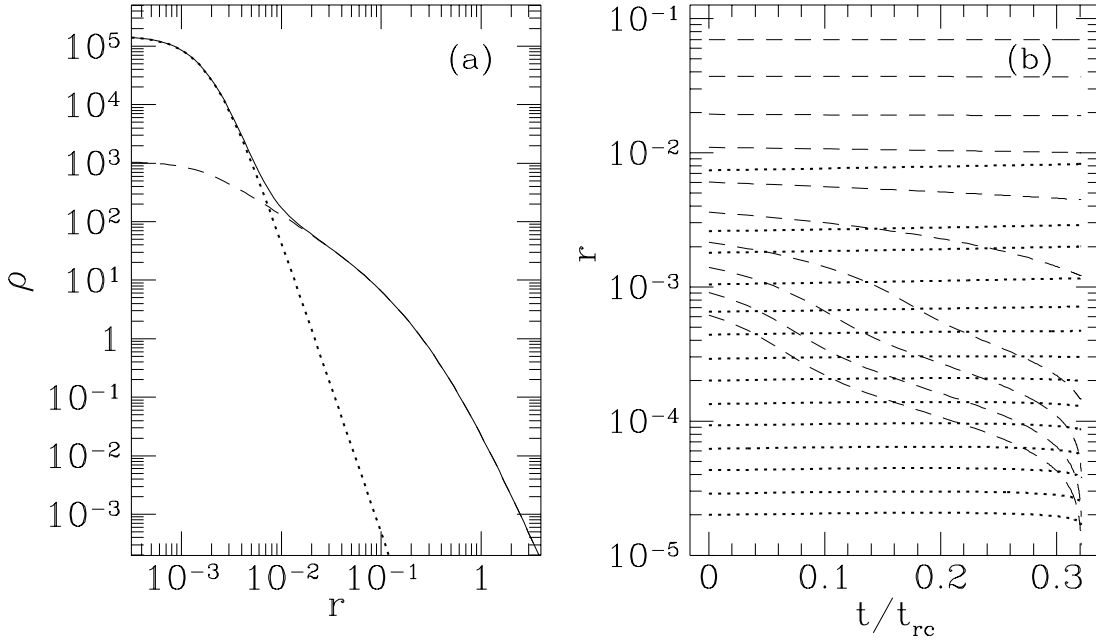


Figure 8: (a) A model formed by combining the densities of a Plummer model with $M_1 = 0.005$ and $R = 0.002$ (dotted line) and a γ model with $\gamma = 1$, $M_2 = 0.995$, $a = 1/3$, and $b = 0.002$ (dashed line). (b) The evolution when $m_2/m_1 = 100$: the dotted lines show radii containing fixed fractions of the mass of the first component (10^{-6} , 3×10^{-6} , 10^{-5} , 3×10^{-5} , ..., 0.1 , 0.3 , 0.5 , 0.9); the dashed lines show the same for the second component (the larger fractions are not visible).

contrived.

4 Applications

4.1 Globular clusters

The importance of relaxation for globular clusters is clear. Most Galactic clusters are fit well by King models—models constructed for relaxed, tidally-truncated star clusters. The majority have concentrations of $W_0 \simeq 6\text{--}8$; fewer than 10% have $W_0 < 4$; about 20% have high concentrations ($W_0 > 10$) or are not fit well by any concentration—these are the “core-collapsed” or “post-core-collapsed” clusters (Trager, King, and Djorgovski 1995). Their fraction is consistent with simple estimates of the collapse rate based on an assumed collapse time that is a fixed multiple of the central relaxation time (Cohn and Hut 1984, Djorgovski and Hut 1992).

In reality the $t_{\text{cc}}/t_{\text{rc}}$ ratio depends on the concentration of a cluster; this can be taken into account. Djorgovski (1993) and Trager et al. (1995) give values of t_{rc} and W_0 (or c) for 124 clusters²; these were combined with the data from Figure 1 to predict the time t_{cc} for each cluster to collapse from its present state, assuming that the clusters are collapsing and that they are isolated, equal-mass King models. Figure 9 shows the resulting distribution. About 20% of the clusters have short collapse times ($t_{\text{cc}} \lesssim 4 \times 10^9$ yr), consistent with the suggestion that many of these have already passed through core collapse (Djorgovski and King 1986).

²Djorgovski’s t_{rh} values are a factor of $\ln(10)$ too small because of an error in his equation (11) (Djorgovski, private communication). The data are available from a catalog maintained by W. E. Harris (at <http://www.physics.mcmaster.ca/Globular.html>).

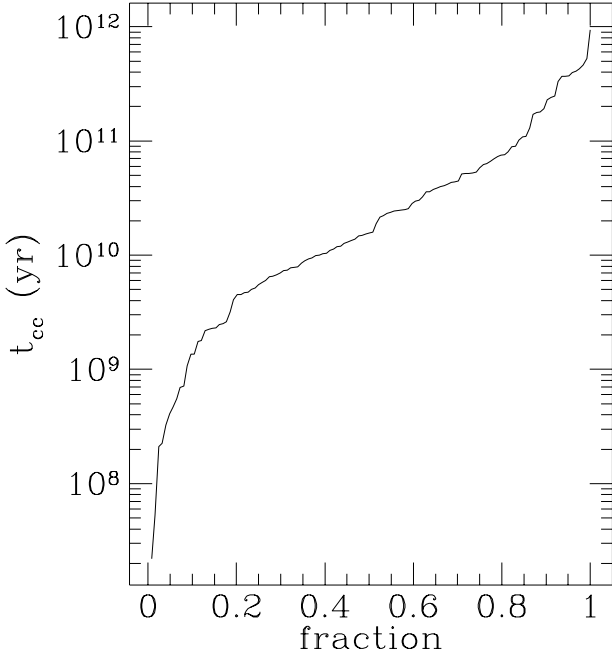


Figure 9: Fraction of Galactic globular clusters with collapse times smaller than t_{cc} .

The collapse times computed here ignore several complicating factors known to be important for real clusters (reviewed by Chernoff 1993), including stellar evolution, mass segregation, and mass loss from a tidal boundary. Stellar evolution always slows the collapse, and can cause some clusters to disrupt; its importance depends on the initial mass function. Mass segregation always accelerates the collapse, by as much as a factor of five or ten for a Salpeter-like mass function (Murphy and Cohn 1988, Chernoff and Weinberg 1990). Mass loss from a tidal boundary is more complicated: if the tidal field is constant, the mass loss accelerates the collapse of low-concentration clusters, by a factor of two or three for $W_0 \lesssim 3$; but if the mass loss is enhanced by gravitational shocks as the clusters pass through the disk or close to the center of the Galaxy, it tends to disrupt low-concentration clusters, though it accelerates the collapse of others. The increase in cluster concentrations towards the center of the Galaxy shows the importance of these environmental factors (Chernoff and Djorgovski 1989, Djorgovski and Meylan 1994). The clusters would have to be modelled on a case by case basis to take all the complications into account; but since they tend mostly to accelerate the collapse it seems that the fraction of clusters with short collapse times is probably larger than shown in Figure 9.

4.2 Galaxies

The relaxation time is known to be short in the centers of several local-group galaxies: about 2×10^7 yr in the nucleus of M33 (Kormendy and McClure 1993); 10^8 yr in the inner 0.5 pc of our Galaxy (Genzel, Hollenbach, and Townes 1994); 4×10^9 yr or 6×10^7 yr in the inner 1 pc of M32, for models with and without massive black holes (Lauer et al. 1992). And short times like these are likely to be common: many galaxies have density cusps that rise as steeply as in our own Galaxy and M32 (Crane et al. 1993, Ferrarese et al. 1994, Forbes et al. 1995, Lauer et al. 1995). If the galaxies are like isotropic γ models (which here includes Zhao's more general class of models), the ones with cusp slopes of $\gamma < 2$ will be expanding. The cusps in those models cannot survive for much longer than the local relaxation time. For distant galaxies the region where the relaxation time is short

cannot be resolved, but for nearby galaxies the consequences of the expansion should be observable.

But it is not clear that real galaxies are like isotropic γ models. The models fit the surface brightness of galaxies well but not the kinematics. Few galaxies show evidence of the temperature inversion that the models predict. The inversion is weakened when the velocity dispersion is projected along the line of sight, but it should still be observable³. The elliptical galaxy NGC 5813 has a dispersion that falls by about 30 km/s towards the center (Efstathiou, Ellis, and Carter 1982), but it does not have an isotropic, power-law cusp: its inner core rotates rapidly and appears to be kinematically distinct; Kormendy (1984) has argued that it is a merger remnant. Five of the forty-four elliptical galaxies in the survey of Bender, Saglia, and Gerhard (1994) have falling central dispersions, but two of these again have rapidly rotating cores (Bender et al. note that $v^2 + v_{\text{rot}}^2$ remains more constant with radius than v^2 does); the other thirty-nine have constant or rising dispersions. Byun et al. (1996) have fit isotropic, power-law cusps to the central regions of fifty-seven elliptical galaxies; the fits for about half predict falling dispersions, yet the data for nearly all show constant or rising dispersions (Tremaine, private communication).

Although the discrepancy between the data and the fits is not large (about 10% on average), it suggests that the galaxies differ from isotropic γ models. It could be that the velocity distributions are not isotropic; a radial bias can raise the dispersion at the center (Tonry 1983). Even if they are isotropic, the dispersion need not fall if there is a steepening density cusp (e.g. Binney 1982) or a rising mass-to-light ratio or a central mass concentration such as a massive black hole. Whatever the reason, relaxation will not change the galaxies as rapidly if their velocity dispersions do not fall because their relaxation times will be longer and their central regions will not be as far out of thermal equilibrium. In galaxies with central black holes the relaxation is enhanced by resonances (Rauch and Tremaine 1996), but this affects only the stars' angular momenta and hence does not lead directly to collapse or expansion.

4.3 Dark star clusters in the centers of galaxies

There is growing evidence for dark mass concentrations in the centers of galaxies, often called massive dark objects (Kormendy and Richstone 1995). They are probably massive black holes, but to make that convincing we must rule out alternatives such as clusters of dark stars (e.g. stellar remnants, brown dwarfs, planets). Various arguments can be made depending on the constraints on the cluster and the assumed mass and size of its stars (Goodman and Lee 1989, Maoz 1995). Here we shall consider only one—that the cluster is unacceptable if it will collapse in a small fraction of its age.

The collapse time is of course unknown because the distribution of mass in the cluster is unknown. But since the goal is to argue that a dark cluster is unacceptable, the collapse time should be chosen in the most generous way to allow for its survival. The best choice is therefore the time for a low-concentration cluster of equal-mass stars, about $10 t_{\text{rh}}$ (where t_{rh} refers to the dark cluster, not to the rest of the galaxy). High-concentration clusters and clusters with a distribution of stellar masses collapse faster than this; high-concentration clusters will suffer from other problems too (as will clusters with density cusps)—their high central densities will lead to stellar collisions and mergers.

Maoz (1995) argued that the massive dark object in NGC 4258 cannot be a cluster of objects of mass $\gtrsim 0.03 M_{\odot}$ because it would collapse in $\lesssim 6$ Gyr. He used for the collapse time an evaporation time of $136 t_{\text{rh}}$; his argument would have been stronger if he had used the time of $10 t_{\text{rh}}$ suggested here (Maoz gave other arguments against a dark cluster). Goodman and Lee (1989) did use a time of $10 t_{\text{rh}}$ in their constraints for M31 and M32, but they assumed that the collapse had been stopped and reversed (by binary heating or mass loss), and argued that $10 t_{\text{rh}}$ could not be much less than the

³The figures of Tremaine et al. (1994) showing the intrinsic and projected dispersions are interchanged: Figure 1 should be Figure 4 and vice versa.

age of an expanding cluster. This is a valid argument if the collapse can be stopped; whether that would happen in M31 and M32 is debatable. At the high velocity dispersions common in galactic nuclei the collapse can continue all the way to the formation of a massive black hole (Quinlan and Shapiro 1989, 1990). Goodman and Lee's constraints are applicable even if the collapse cannot be stopped, however, because a dark cluster is unacceptable whether collapsing or expanding if $10 t_{\text{rh}}$ is much less than its age.

The collapse time for a dark cluster can be made arbitrarily long by giving its stars an arbitrarily small mass, and the problems with collisions and mergers can be avoided by assuming the "stars" to be elementary particles or small black holes. But then the cluster can capture stars from the rest of the galaxy and cause them to collapse in a short time (as happened in the model in Fig. 8). This gives another constraint on the size of the cluster, because if too many stars get captured they might collapse to a massive black hole, making the cluster an unacceptable alternative.

Acknowledgements

I thank Martin Rees for suggesting the importance of mass segregation in models like that shown in Figure 8, and Douglas Heggie, Tad Pryor, Scott Tremaine, and Martin Weinberg for helpful discussions about other parts of the work. Financial support was received from NSF grant ASC 93-18185 at UCSC and from NSF grant AST 93-18617 and NASA Theory grant NAG 5-2803 at Rutgers.

A Calculations with variable Coulomb logarithm

The perturbations to a star's energy from stars with different impact parameters combine in such a way that, in a homogeneous cluster, equal logarithmic intervals in impact parameter contribute equal amounts. This is the origin of the Coulomb logarithm,

$$\ln \Lambda = \ln(b_{\text{max}}/b_{\text{min}}) = \ln(v^2 b_{\text{max}}/Gm), \quad (11)$$

with b_{min} the impact parameter corresponding to a 90-degree deflection. For low-concentration clusters b_{max} is usually taken to be the size of the cluster (Farouki and Salpeter 1995); then $\Lambda = kN$ with $k \simeq 0.4$ (k is used here instead of the usual γ to avoid confusion with the γ models). Giersz and Heggie (1994) found that $k = 0.11$ works better than $k = 0.4$ when N-body experiments and Fokker-Planck and gas-model calculations are compared for the collapse of a Plummer model, perhaps because of the contribution from non-dominant terms in the perturbation integrals (Hénon 1975). This difference will be ignored here. For high-concentration clusters it is not clear that any value of k will work well because equal logarithmic intervals in impact parameter do not contribute equal amounts when the density varies with radius. Binney and Tremaine (1987, p. 511) suggest that for such clusters b_{max} should be the radius of a star's orbit. Giersz and Heggie (1994) used a similar choice in some of their gas-model calculations—they took $\Lambda(r) \sim \text{Max}\{N_c, N(r)\}$ and found that it slowed the collapse (they did not say by how much).

The variation of the Coulomb logarithm with radius can be included in the Fokker-Planck equation by including the logarithm in the integrals that result from the orbit-averaging process. The p and q integrals in the definitions of D_E and D_{EE} (eqns. 2 and 3) must be replaced by

$$p_\Lambda(E) = \frac{\partial q_\Lambda}{\partial E}, \quad q_\Lambda(E) = \frac{1}{3} \int_0^{\phi^{-1}(E)} dr r^2 [2(E - \phi)]^{3/2} \ln \Lambda(r); \quad (12)$$

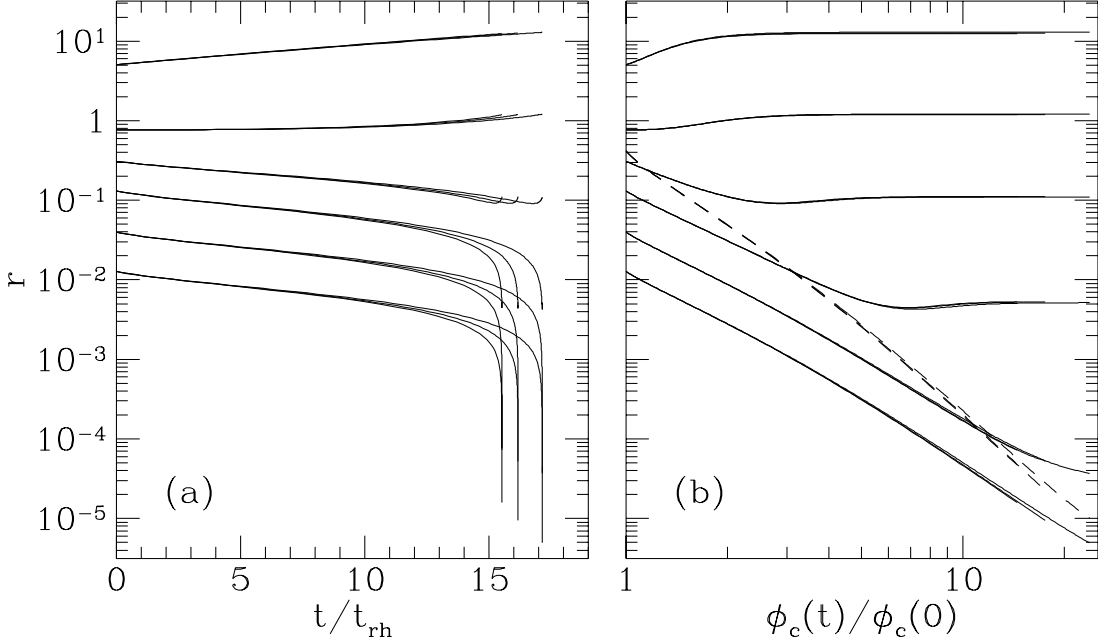


Figure 10: Collapse of a Plummer model with a Coulomb logarithm that depends upon radius. The solid lines are radii containing fixed fractions of the total mass ($10^{-5}, 3 \times 10^{-4}, 10^{-2}, 0.1, 0.5, 0.9$); the dashed line is the core radius. There are three sets of lines, for $N = 10^4$ (the slowest collapse), 10^8 , and ∞ (the fastest collapse).

the p and q in equation (1) are not changed. In the experiments described below $\Lambda(r)$ was taken to be

$$\Lambda(r) = \frac{Nv^2(r)}{GM} \text{Max}\{r, r_c\}. \quad (13)$$

For a Plummer model this gives $\Lambda \simeq 0.5N$ in the halo and $\Lambda \simeq 0.35N$ in the core, close to the usual choice of $0.4N$. The value of N must be specified at the start of the calculation; it cannot be absorbed into the unit of time as it can when a constant logarithm is used.

Figure 10 compares the evolution of Plummer models computed using two values of N (10^4 and 10^8) and using a constant Coulomb logarithm (which corresponds to $N = \infty$). Energy and mass were conserved as well with the variable logarithm as with the constant logarithm. The main difference between the calculations is the collapse time, with t_{cc}/t_{rh} equal to 17.1, 16.1, and 15.4 for $N = 10^4$, 10^8 , and ∞ (t_{rh} is computed from the usual definition with $k = 0.4$; the t_{cc}/t_{rh} values change slightly if a different choice is made for k). The difference between the calculations is much smaller if the results are compared at the same central potential instead of at the same time. The three sets of lines in panel (b) lie almost on top of each other; the only difference noticeable is that the core radius does not fall as rapidly with the potential near the end of the calculation with $N = 10^4$ as it does with the other two N values. The collapse rate, $\xi = t_{rc} d\rho_c/dt$, has about the same value during the three calculations if the appropriate value for Λ in the core is used in the definition of t_{rc} (although near the end ξ is slightly larger with $N = 10^4$ than with the other two N values).

Calculations done with γ models gave similar results. The evolution is slower when the Coulomb logarithm varies with radius because the relaxation time near the center is then longer, but the difference is large only at radii where $\Lambda \simeq 1$. For most time-scale estimates it can be allowed for by evaluating Λ at the radius where it is needed. The one exception might be detailed comparisons of N-body experiments with Fokker-Planck or gas-model calculations; small changes to the collapse

time can be important for that. There are of course factors besides the Coulomb logarithm that can cause such changes (Giersz and Heggie 1994, Giersz and Spurzem 1994).

References

Bender, R., Saglia, R. P., and Gerhard, O. E. 1994, Line-of-sight velocity distributions of elliptical galaxies, *MNRAS* **269**, 785–813.

Binney, J. 1980, The radius-dependence of velocity dispersion in elliptical galaxies, *MNRAS* **190**, 873–880.

Binney, J. 1982, The phase space structure of $r^{1/4}$ galaxies: are these galaxies ‘isothermal’ after all?, *MNRAS* **200**, 951–964.

Binney, J. and Tremaine, S. 1987, *Galactic Dynamics*, Princeton Univ. Press.

Byun, Y.-I. et al. 1996, The centers of early-type galaxies with HST. II. Empirical models and structural parameters, *AJ*, **111**, 1889–1900.

Carollo, C. M. 1993, *Structure of Elliptical Galaxies, Line-strengths, Kinematics and Dynamics*, PhD thesis, Ludwig-Maximilians Univ. Munich.

Chernoff, D. F. 1993, A review of fundamental issues in the evolution of globular clusters in the Galaxy, in *Structure and Dynamics of Globular Clusters*, edited by Djorgovski, S. G. and Meylan, G., pp. 245–262 (ASP Conference Series).

Chernoff, D. F. and Djorgovski, S. 1989, An analysis of the distribution of globular clusters with postcollapse cores in the Galaxy, *ApJ* **339**, 904–918.

Chernoff, D. F. and Weinberg, M. D. 1990, Evolution of globular clusters in the Galaxy, *ApJ* **351**, 121–156.

Cohn, H. 1980, Late core collapse in globular clusters and the gravothermal instability, *ApJ* **242**, 765–771.

Cohn, H. 1985, Direct Fokker-Planck calculations, in *Dynamics of Star Clusters*, edited by Goodman, J. and Hut, P., pp. 161–178 (D. Reidel, Dordrecht).

Cohn, H. and Hut, P. 1984, Is there life after core collapse in globular clusters?, *ApJ* **277**, L45–L48.

Cohn, H., Hut, P., and Wise, M. 1989, Gravothermal oscillations after core collapse in globular cluster evolution, *ApJ* **342**, 814–822.

Crane, P. et al. 1993, High resolution imaging of galaxy cores, *AJ* **106**, 1371–1393.

Dehnen, W. 1993, A family of potential-density pairs for spherical galaxies and bulges, *MNRAS* **265**, 250–256.

Djorgovski, S. 1993, Physical parameters for Galactic globular clusters, in *Structure and Dynamics of Globular Clusters*, edited by Djorgovski, S. G. and Meylan, G., pp. 373–382 (ASP Conference Series).

Djorgovski, S. and Hut, P. 1992, Rates of collapse and evaporation of globular clusters, *Nature* **359**, 806–808.

Djorgovski, S. and King, I. R. 1986, A preliminary survey of collapsed cores in globular clusters, *ApJ* **305**, L61–L65.

Djorgovski, S. and Meylan, G. 1994, The Galactic globular cluster system, *AJ* **108**, 1292–1311.

Efstathiou, G., Ellis, R. S., and Carter, D. 1982, Further observations of the elliptical galaxy NGC 5813, *MNRAS* **201**, 975–990.

Farouki, R. T. and Salpeter, E. E. 1995, Mass segregation, relaxation, and the Coulomb logarithm in N-body systems (again), *AJ* **427**, 676–683.

Ferrarese, L., van den Bosch, F. C., Ford, H. C., Jaffe, W., and O’Connell, R. W. 1994, Hubble Space Telescope photometry of the central regions of Virgo cluster elliptical galaxies. III. Brightness profiles, *AJ* **108**, 1598–609.

Forbes, D. A., Franx, M., and Illingworth, G. D. 1995, Ellipticals with kinematically distinct cores: WFPC1 imaging of nearby ellipticals, *AJ* **109**, 1988–2002.

Genzel, R., Hollenbach, D., and Townes, C. H. 1994, The nucleus of our Galaxy, *Rep. Prog. Phys.* **57**, 417–479.

Giersz, M. and Heggie, D. C. 1994, Statistics of N-body simulations. I. Equal masses before core collapse, *MNRAS* **268**, 257–275.

Giersz, M. and Spurzem, R. 1994, A comparison of direct N-body integration with anisotropic gaseous models of star clusters. *MNRAS* **269**, 241–256.

Goodman, J. 1983, Core collapse with strong encounters, *ApJ* **270**, 700–710.

Goodman, J. 1989, Late evolution of globular clusters, in *Dynamics of Dense Stellar Systems*, edited by Merritt, D., pp. 183–193 (Cambridge Univ. Press).

Goodman, J. 1993, The theory of pre- and post-core-collapse evolution and gravothermal oscillations, in

Structure and Dynamics of Globular Clusters, edited by Djorgovski, S. G. and Meylan, G., pp. 87–99 (ASP Conference Series).

Goodman, J. and Lee, H. M. 1989, Black holes or dark clusters in M31 and M32?, *ApJ* **337**, 84–90.

Heggie, D. C., Inagaki, S., and McMillan, S. L. W. 1994, Gravothermal expansion in an N-body system, *MNRAS* **271**, 706–718.

Heggie, D. C. and Mathieu, R. D. 1986, Standardised units and time scales, in *The Use of Supercomputers in Stellar Dynamics*, edited by Hut, P. and McMillan, S. L. W., pp. 233–235 (Springer-Verlag, Berlin).

Heggie, D. C. and Ramamani, N. 1989, Evolution of star clusters after core collapse, *MNRAS* **237**, 757–783.

Hénon, M. 1975, Two recent developments concerning the Monte Carlo method, in *Dynamics of Stellar Systems*, edited by Hayli, A., pp. 133–149 (Reidel, Dordrecht).

Hernquist, L. 1990, An analytical model for spherical galaxies and bulges, *ApJ* **356**, 359–364.

Jaffe, W. 1983, A simple model for the distribution of light in spherical galaxies, *MNRAS* **202**, 995–999.

Katz, J. 1980, Stability limits for ‘isothermal’ cores in globular clusters, *MNRAS* **190**, 497–507.

King, I. R. 1966, The structure of star clusters. III. Some simple dynamical models, *AJ* **71**, 64–75.

Kormendy, J. 1984, Recognizing merger remnants among normal elliptical galaxies: NGC 5813, *ApJ* **287**, 577–585.

Kormendy, J. and McClure, R. D. 1993, The nucleus of M33. *AJ* **105**, 1793–1812.

Kormendy, J. and Richstone, D. 1995, Inward bound - the search for supermassive black holes in galactic nuclei, *Ann. Rev. Astron. Astrophys.* **33**, 581–624.

Lauer, T. R. et al. 1992, Planetary Camera observations of the central parsec of M32, *AJ* **104**, 552–562.

Lauer, T. R. et al. 1995, The centers of early-type galaxies with HST. I. An observational survey, *AJ* **110**, 2622–2654.

Makino, J. 1996, Gravothermal oscillations, in *Dynamical Evolution of Star Clusters*, edited by Hut, P. and Makino, J., in press (Kluwer).

Maoz, E. 1995, A stringent constraint on alternatives to a massive black hole at the center of NGC 4258, *ApJ* **447**, L91–L94.

Murphy, B. W. and Cohn, H. N. 1988, Realistic models for evolving globular clusters: core collapse with a mass spectrum, *MNRAS* **232**, 835–852.

Quinlan, G. D. and Shapiro, S. L. 1989, Dynamical evolution of dense clusters of compact stars, *ApJ* **343**, 725–749.

Quinlan, G. D. and Shapiro, S. L. 1990, The dynamical evolution of dense star clusters in galactic nuclei, *ApJ* **356**, 483–500.

Rauch, K. P. and Tremaine, S. 1996, Resonant relaxation in stellar systems, *NewA*, in press.

Spitzer, L. 1987, *Dynamical Evolution of Globular Clusters*, Princeton Univ. Press.

Spurzem, R. and Aarseth, S. 1996, Direct collisional simulation of 10000 particles past core collapse, *MNRAS*, in press.

Takahashi, K. 1995, Fokker-Planck models of star clusters with anisotropic velocity distributions. I. Pre-collapse evolution, *PASJ* **47**, 561–573.

Tonry, J. L. 1983, Anisotropic velocity dispersions in spherical galaxies, *ApJ* **266**, 58–68.

Trager, S. C., King, I. R., and Djorgovski, S. 1995, Catalogue of Galactic globular-cluster surface-brightness profiles, *AJ* **109**, 218–241.

Tremaine, S. et al. 1994, A family of models for spherical stellar systems, *AJ* **107**, 634–644.

Wiyanto, P., Kato, S., and Inagaki, S. 1985, Evolution of single-component King clusters, *PASJ* **37**, 715–726.

Zhao, H. S. 1996, Analytical models for galactic nuclei, *MNRAS* **278**, 488–496.